Earth Reinforcement Practice, Ochiai, Hayashi & Otani (eds) © 1992 Balkema, Rotterdam. ISBN 90 5410 093 1

Experimental study on full scale geogrid reinforced embankment model

H.Miki & K.Kudo
Public Works Research Institute, Ministry of Construction, Japan
M.Taki & N.Fukuda
Fukken Co., Ltd, Japan
K.Iwasaki & J.Nishimura
Mitsui Petrochemical Industries Ltd, Japan

ABSTRACT: A full scale embankment (height 6.25 m, front slope 1:0.2, fill material: dry sand) is constructed by reinforcing with geogrids and these are successively disconnected by passing electricity through the nichrome wires which are prewound in advance. With the decrease of the number of geogrids the embankment gradually loses the stability and finally collapses when all the geogrids are disconnected. It was learned from the experiment that the effects of the pseudo retaining wall (width 70 cm) formed by the pile of sandbags sandwiched by geogrids on the front slope is required to be taken into consideration in the stability analysis of the embankment. Analyses and discussion were made in this paper, placing emphasis on evaluation of the efficiency of slope protection structures, sandwiched by sandbags and geogrids, acting as a wall structure.

1. INTRODUCTION

The importance of slope protection structures, provided for stabilizing reinforced embankment, is acknowledged by a number of researchers and has been pointed out by various research institutions. Experiments were made to resolve the integrating mechanism of embankments by cutting geogrids and gradually opening the horizontal spaces of geogrids. As a result, it could be found that the integrated zone (70 cm in depth from the surface) within the slope acted as a pseudo retaining wall and contributed greatly for stabilizing the embankment. Therefore, analyses and discussion were made in this paper, placing emphasis on evaluation of the efficiency of slope protection structures, sandwiched by sandbags and geogrids, acting as a wall structure.

2. METHODS OF EXPERIMENT

(1) Reinforced embankment

The reinforced embankment, shown in Figure 1, was constructed 6.25 m high and 5 m wide, with a slope gradient of 1 : 0.2. A geogrid was laid out on each 25 cm lift of the embankment fill. Sandbags (45 cm in width and 12.5 cm thick) were piled on the sloped embankment surface, placing geogrids between every two sandbags. The conventional folding method was not applied in this experiment.

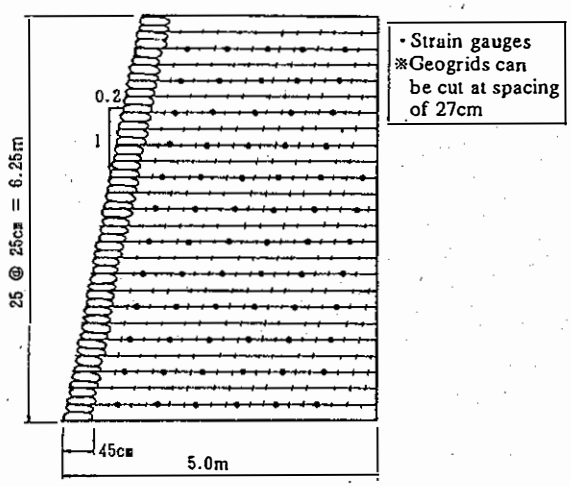

Fig. 1 Cross sectional view of reinforced embankment

(2) Materials

Embankment was filled with dry sand with a water content of 2.9%, reduced to a minimum to retain cohesion, and were compacted to a

thickness of 25 cm for each lift with a 60-kg tamper. Soil was compacted to an average density of 1.63 g/cm³ (approximately 94% of maximum density), and had a strength of c = 0.2 tf/m² and ϕ = 41°, measured by a triaxial CD test (unsaturated condition). Geogrid used for the experiment, had been certified to have a maximum tensile strength of 4.5 tf/m and an maximum elongation of approximately 17%.

(3) Experiment procedures

It was decided to cut the geogrid at a spacing of 27 cm, as shown in Figure 1, to delete the reinforcing effect of the material. The geogrid was cut in the order shown in Figure 2. The spacing of geogrid was 0.25 m at the time the embankment was constructed but reduced to 1.0 m and 2.0 m at cutting stages ② and ③. Lengthwise cutting started at stage ④. At the end of the cutting process the wall structure was formed of a sloped surface of sandbags (and partially of embankment fiII) 70 cm wide, sandwiched with geogrid. Measurements were made to read the strains of the geogrid. (at a spacing of 60 cm), the horizontal displacement of the slope, and the settlement of the top of the embankment. Strain gauges that can read elongations up to 10% were used to measure strain.

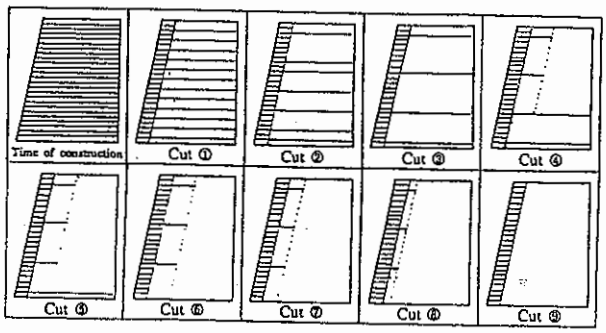

Fig. 2 Cutting stages of geogrid

3. RESULTS OF EXPERIMENTS

(1) Displacement of embankment

Figure 3 shows the displacement of the embankment and strains occurring in the geogrid. Gradual displacement and strain readings occurred at cutting stages ① and ② slightly rising at cutting stage ③. However, measured maximum horizontal displacement, settlement of ground, and strain were 1.5 cm, 0.6 cm, and 2.0% respectively. At this point of time the line connecting the peak strains of the geogrid approximated the circular slip assumed in pre-analysis. It could be seen that stresses within the embankment were redistributed and that the slope stability changed as the reinforcement was reduced.

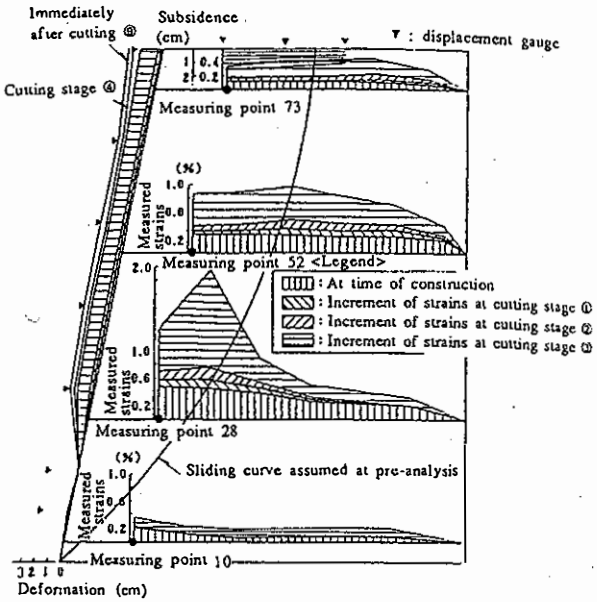

Fig. 3 Displacement of embankment and strains occurring in geogrid

Conversely, the increments of displacement and strains quickly decreased after cutting stage ④ and did not show significant changes from cutting stage ⑨ to the final stage of collapse. The strains of the geogrid showed a tendency to decrease at most points, except for a very limited area (the area around measuring point 28). It can be assumed that the reinforcing effect of the geogrid remaining in the embankment did not increase.

The embankment completely collapsed two hours after the geogrid was cut at stage ⑨.

(2) Estimation of collapsing process

Collapsing patterns, assumed from the shape of the collapsed embankment and from field verification conducted on the slip surface by test excavations, are shown in Figure 4. It can be assumed that the collapse had occurred first with an initial overturn at the toe of the slope, and followed with slipping of the rear embankment. It can be estimated that the rigidity of the wall structure was small compared with the lateral

structure was small compared with the lateral earth pressure or horizontal sliding force of embankment.

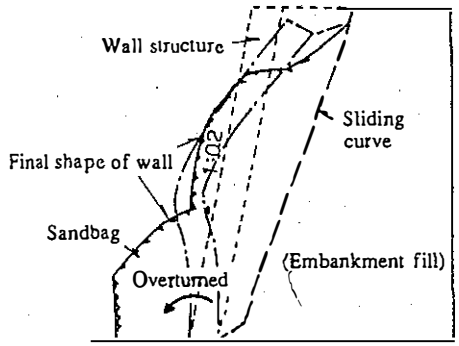

Fig. 4 Collapsing patterns of embankment

4. ANALYSES

4.1 Determination of safety factors by conventional methods

Safety factors of the embankment, using measured tensile strength of the geogrid, will be calculated using the circular slip method and the trial wedge method, both of which are currently being used in design. The effect of wall structures has not been considered in these conventional methods. Safety factors (FS) can be defined with equations shown below:

(a) Circular slip safcty factor, $FS = \dfrac{M_R + \Delta M_R}{M_D}$

In the above, M_D = sliding moment, M_R = resisting moment of soil, ΔM_R = resisting moment of geogrid, $\Delta M_R = R\Sigma Ti$, R = radius of slip circle, and ΣTi = sum of tensile strengths of geogrid.

(b) Trial wedge safety factor, $FS = \dfrac{\Sigma Ti}{P_H}$

In the above, P_H = horizontal earth pressure and ΣTi = sum of tensile strengths of geogrid..

Experiment procedures and the transition of safety factors are shown in Figure 5. From the figure, it can be seen that there are differences in absolute values of safety factors for circular slip and trial wedge methods, because of different definitions. Both safety factors are less than 1.0 at cutting stage ③. The safety factor by circular slip method is 0.62 without reinforcement (cutting stage ⑥ and later). Therefore, there are significant differences between current design methods and the experiment data.

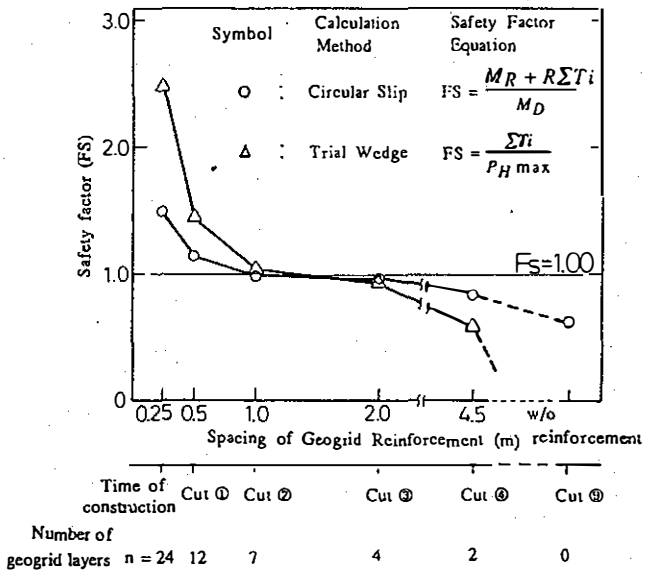

Fig. 5 Determination of safety factors based on measured tensile strength of geogrid

4.2 Determining acting force of wall structure assumed as a pseudo retaining wall

It will be necessary to analyze the behavior of the wall structure (sectional area of the slope to a depth of 70 cm in this case), which is not normally done with conventional stability analyses. In the following analyses, the whole wall structure will be assumed to act as a pseudo retaining wall. Stability analyses will determine safety factors by the circular slip method, horizontal earth pressure by the trial wedge method, and stability against overturning of the pseudo retaining wall by the force polygon method.

When the wall structure is assumed to be a rigid structure, acting force such as shown in Figure 6 would occur from the dead weight of wall structure. External forces horizontally acting on the embankment can be obtained by balancing moments at point O, the toe of retaining wall, as shown in the following equation. The external force acting horizontally was assumed to be acting at a point one third of the total height of the retaining wall.

$$W \cdot x = P \cdot H/3$$
$$x = n \cdot H/2 + b/2$$
$$\therefore P = 3W\,(n/2 + b/2H) \quad \ldots\ldots\ldots\ldots (1)$$

Where, P = horizontal resistance of wall structure acting on embankment (tons), W = weight of wall (tons), H = height of wall (m), b = width of wall base, and n : gradient of sloped wall. Bearing strength and safety for sliding must be ensured at the bottom of wall.

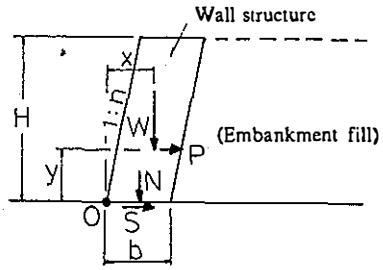

Fig. 6 Acting force of retaining wall

4.3 Determination of safety factors considering resistance of wall structure

When an external pressure acts horizontally, the circular slip safety factor of the embankment can be obtained by the following equation. Symbols are shown in Figure 7.

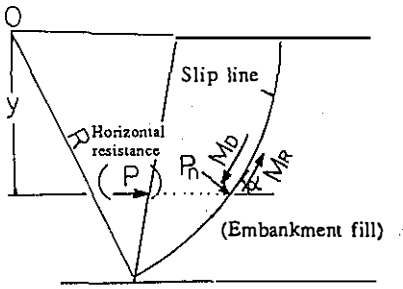

Fig. 7 Circular slip safety factor

$$F_S = (M_R + \Delta M_R) / M_D \quad \cdots\cdots\cdots\cdots (2)$$
$$\Delta M_R = P \cdot y$$

In the above equation, F_S = circular slip safety factor, M_R = resisting moment of embankment, ΔM_R = resisting moment of wall structure, M_D = sliding moment, P = horizontal resistance of wall structure, and y = vertical distance between the center of circular arc and the point where P acts.

Slip surfaces in the trial wedge method can be assumed to be two straight-line slips caused by the horizontal earth pressure, similar to the experiment data. Total horizontal earth pressure components (P_H) of the two straight-line slips, divided into two areas, zone ① and zone ②, as shown in Figure 8, can be obtained based on the concept of force polygons. It can be determined that the embankment is stable when the external force of retaining wall acting is larger than P_H.

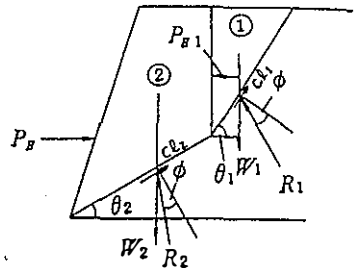

(a) General View

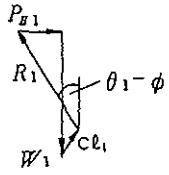

(b) Balancing of Zone ①

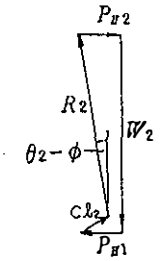

(c) Balancing of Zone ②

Fig. 8 Determining horizontal earth pressure by trial wedge method

Figure 9 shows the experimental procedures and the safety factors considering resistance of wall structure. This figure has been developed from Figure 5, taking into consideration the resisting strength of the wall structure. It can be seen that the figure indicates a behavior nearly equal to the behavior obtained by experiments, when compared with Figure 5.

4.4 Examination on overturn of retaining walls by force polygon method

Stability of pseudo retaining walls for overturning will be examined using the force polygon method proposed for masonry retaining walls. Applied point of resultant force, consisting of wall structure weight and earth pressure, can be obtained by the following equation (see Fig. 10), if earth pressure can be assumed to act horizontally. The time when point "M" in Figure 10 acts on the external side of wall structure section can be deemed as an overturn.

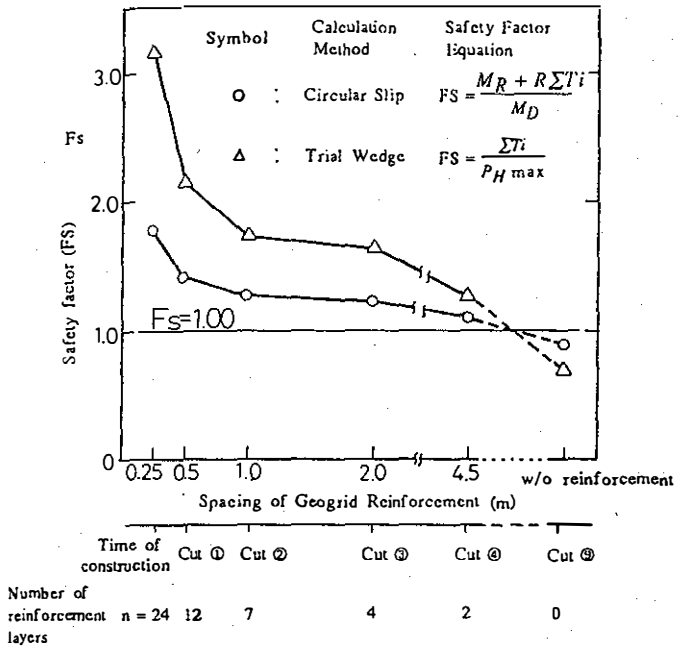

Fig. 9 Transition of safety factors based on measured tensile strength, taking into consideration the wall structure

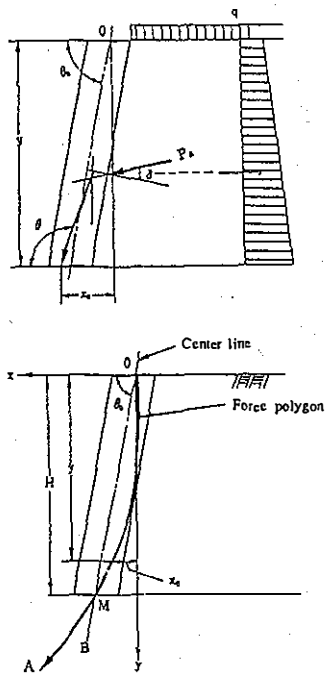

Fig. 10 Determining applied point of resultant force by force polygon method

$$x_0 = \frac{Ka \cdot \gamma}{6\gamma_s \cdot b\sqrt{1+\cot^2\theta_0}} y^2 + \left(\frac{Ka \cdot q}{2\gamma_s \cdot b\sqrt{1+\cot^2\theta_0}} + \frac{\cot\theta_0}{2}\right) y \quad \cdots\cdots (3)$$

Where, x_0 and y : horizontal and vertical distances (m) from top center of wall structure to the point where resultant force is applied, Ka : coefficient of earth pressure, γ and γ_s : unit volume weight of backfill and wall structure (t/m³), q : applied load (t/m²).

Figure 11 shows the force polygon where the wall thickness is assumed to be 70 cm. The critical height of the embankment against overturning (Hc), obtained by force polygon, was 5.75 m. The corresponding cohesion, where $Hc = 6.25$, was $c = 0.27$ tf/m². The figure shows two different cases, where the gradient of slope is assumed to be 1 : 0 (case 2) and 1 : 0.4 (case 3). It can be seen that the wall appears to overturn forward in case 2, and tends to lean backward in case 3, compared with the actual status (case 1).

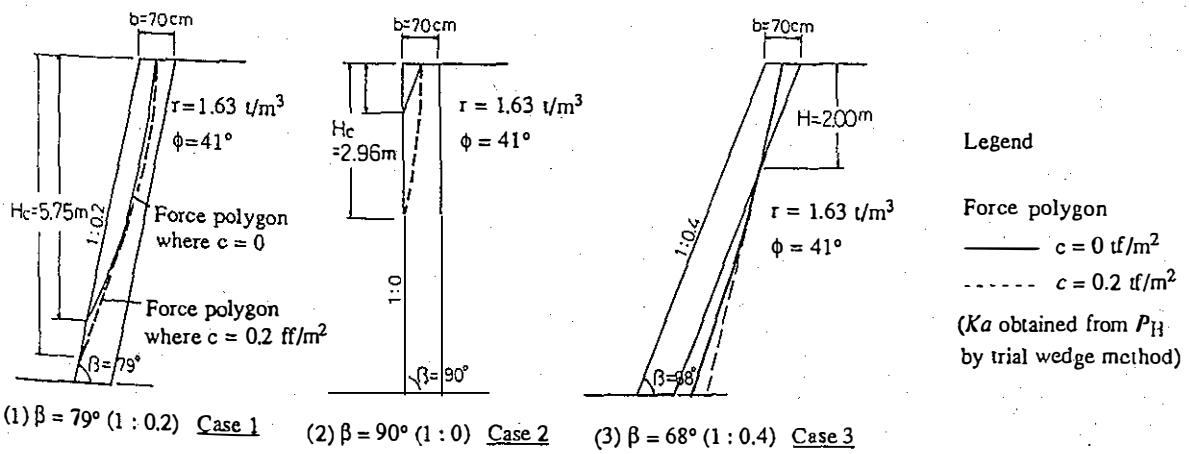

Fig. 11 Force Polygon (b = 0.70 m, $\phi = 41°$, slope gradient = 1:0.2, 1:0, 1:0.4)

5. DISCUSSION

Figure 12 shows the changes in proportion of sharing the resistance forces against sliding force, reviewed from the standpoint of reverse analyses by circular slip method made at $F_S = 1.00$, assuming that reinforced embankments are stabilized when the sliding force of earth mass (F_D), shearing resistance of soil (F_{RS}), the reinforcing strength of geogrids (F_{RG}), and the reinforcing strength of wall structure (F_{RW}) are all balanced at each cutting step. The slip circular which most lacks the resistance force ($F_{RG} + F_{RW}$) and the measured values for F_{RG} on its slip line were used as balancing conditions here. In order to determine F_D and F_{RS}, the shearing resistance angle of soil (ϕ'_{mob}) was assumed to change, and trial calculations were repeated until all strengths have been balanced at $F_S = 1.00$.

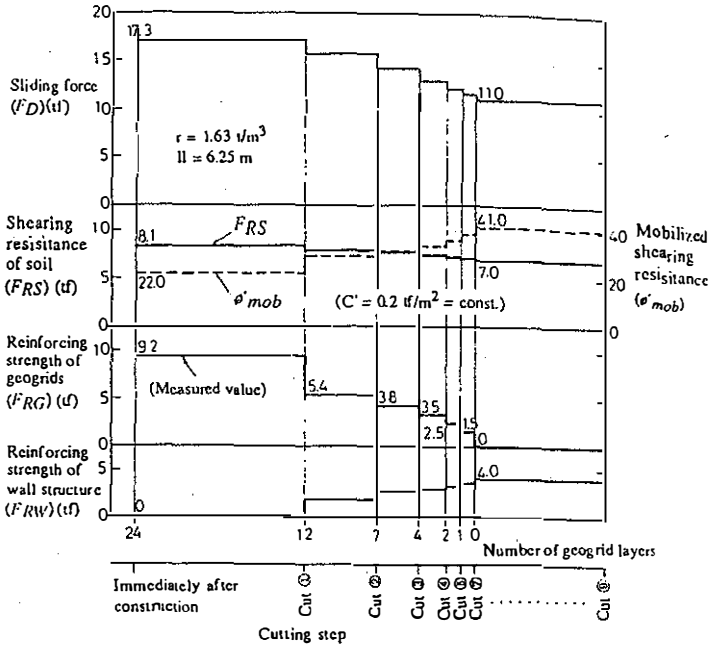

Fig. 12 Relationship between cutting steps, and sliding force of soil mass, shearing resistance of soil, and reinforcing strength of geogrids and wall structure

It can be seen from the figure that the shearing resistance of soil (F_{RS}) and reinforcing strength of geogrids (F_{RG}) were fully resisting the sliding force, and the reinforcing strength of wall structure (F_{RW}) was not exhibiting before cutting of geogrids started, but the reinforcing strength of geogrids reduced and the reinforcing strength of wall structure increased as cutting proceeded. It can also be seen that a considerably large portion of the total resistance force in approximately 35% had been shared by the wall structure immediately before the embankment collapsed.

6. CONCLUSION

As a result of experiments made for a full scale embankment reinforced with geogrids that were prewound with nichrome wires, which were gradually cut by electric current, it has been learned that the slope protection of wall structure, sandwiched by sandbags and geogrids, exhibits great effects. Analyses were made for the effects of slope protection of wall structure, using methods of calculation assuming the slope protection to be a pseudo retaining wall, as described in chapters 4 and 5, and quantitative analyses were made for the mechanism of resistance forces yielded by slope protection.

Continued efforts will be made to propose design procedures for reinforced embankments, incorporating the effects of slope protection in the next chance.

REFERENCES

Miki, H. et al. 1991. *Experimental Study on Full Scale Geogrid Reinforced Embankment Model*, The 44th Annual Symposium at Japan Society of Civil Engineers, pp. 774 - 775.